Ferroferric Oxide/Multiwalled Carbon Nanotube vs Polyaniline/Ferroferric Oxide/Multiwalled Carbon Nanotube Multiheterostructures for Highly Effective Microwave Absorption

Mao-Sheng Cao,*,[†] Jian Yang,[†] Wei-Li Song,*,[†] De-Qing Zhang,[‡] Bo Wen,[†] Hai-Bo Jin,[†] Zhi-Ling Hou,[†] and Jie Yuan*,[†,§]

[†]School of Materials Science and Engineering, Beijing Institute of Technology, Beijing 100081, P. R. China
[‡]School of Chemistry and Chemical Engineering, Qiqihaer University, Qiqihaer 161006, P. R. China
[§]School of Information Engineering, Minzu University, Beijing 100081, P. R. China

ABSTRACT: Light-weight nanocomposites filled with carbon nanotubes (CNTs) are developed for their significant potentials in electromagnetic shielding and attenuation for wide applications in electronics, communication devices, and specific parts in aircrafts and vehicles. Specifically, the introduction of a second phase into/onto CNTs for achieving CNT-based heterostructures has been widely pursued due to the enhancement in either dielectric loss or magnetic loss. In this work, ferroferric oxide (Fe_3O_4) was selected as the phase in multiwalled carbon nanotube (MWCNT)-based composites for enhancing magnetic properties to obtain improved electromagnetic attenuation. A direct comparison between the two-phase heterostructures (Fe_3O_4/MWCNTs) and polyaniline (PANI) coated Fe_3O_4/MWCNTs, namely, three-phase heterostructures (PANI/Fe_3O_4/MWCNTs), was made to investigate the interface influences of Fe_3O_4 and PANI on the complex permittivity and permeability separately. Compared to PANI/Fe_3O_4/MWCNTs, Fe_3O_4/MWCNTs exhibited enhanced magnetic properties coupled with increased dielectric properties. Interfaces between MWCNTs and heterostructures were found to play a role in the corresponding properties. The evaluation of microwave absorption of their wax composites was carried out, and the comparison between Fe_3O_4/MWCNTs and PANI/Fe_3O_4/MWCNTs with respect to highly efficient microwave absorption and effective absorption bandwidth was discussed.

KEYWORDS: carbon nanotube, ferroferric oxide, polyaniline, heterostructure, microwave absorption
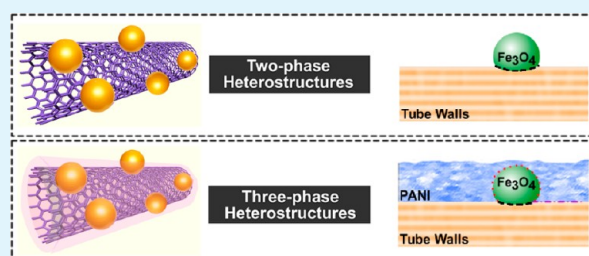
INTRODUCTION

Lightweight nanocomposites of high-performance electromagnetic shielding and attenuation properties promise great applications with examples ranging from cutting edge electronics to specific devices in aircrafts and vehicles.[1-5] Among the pursued nanoscale fillers, carbon nanotubes (CNTs) have attracted extensive development effort for their both mechanical and electrical properties.[6,7]

Upon the low percolation threshold and excellent dielectric/electrical loss,[8-10] neat CNTs embedded into polymer matrices have already demonstrated dramatically enhanced electromagnetic shielding and attenuation in the resulting polymeric nanocomposites.[1,2,11-13] Among widely studied polymeric matrices, polyaniline (PANI), polymerized from the inexpensive aniline monomer, has aroused interest because of the change in electrical conductivity based on different oxidation states.[12] At this point, electrically conductive PANI has been considered as an ideal matrix or the second phase incorporated with CNTs for unique electromagnetic shielding and attenuation.[14] In recent years, various strategies, such as introduction of metals into/onto CNTs,[15-22] have been explored to improve magnetic properties for achieving enhanced electromagnetic shielding and attenuation performance by both dielectric and magnetic

loss. For examples, Che and coworkers[18] reported enhancement in the microwave absorption of Fe encapsulated within carbon nanotubes, which has been proposed to be mainly influenced by magnetic effects from the confinement of Fe. Wen and coworkers[19] fabricated multiwalled carbon nanotube (MWCNT)/Fe, MWCNT/Co, and MWCNT/Ni nanopowders and investigated their microwave absorption properties, demonstrating enhanced microwave absorption properties due to proper combination of the complex permittivity and permeability deriving from MWCNTs and the magnetic nanoparticles. Zhao and coworkers[20] fabricated Fe-filled carbon nanotubes with dramatic improvement of microwave absorption. Kim et al.[21] synthesized MWCNT-PMMA composites containing Fe catalyst, which has been put forward to be used for EMI shielding materials.

Beyond these two-phase structures, a variety of experimental approaches have been developed and practiced for the synthesis of multiple-phase structures based on carbon nanotubes for certain purposes in electromagnetic shielding and attenu-

ation.[8,23,24] For instance, in the work by Dang and coworkers,[8] three-phase BaTiO$_3$-carbon nanotube/polyvinylidene fluoride composites were fabricated, with significantly enhanced dielectric constant and gradually decreased loss. Zhao and coworkers[23] prepared Fe$_3$O$_4$ decorated multiwalled carbon nanotube hybrids using poly(N-vinyl-2-pyrrolidone) as dispersant, demonstrating strong microwave absorption and potential applications. Yun and coworkers[24] synthesized polyaniline-coated MWCNT/γ-Fe$_2$O$_3$ nanocopposites, showing significant improvement in permittivity, permeability, and electromagnetic interference shielding efficiency.

Here in this report, paraffin wax was selected as the host for the nanocomposites embedded with ferroferric oxide/multi-walled nanotubes (Fe$_3$O$_4$/MWCNTs, two-phase heterostructures) (scheme 1) *vs* polyaniline/ferroferric oxide/multiwalled

Scheme 1. Illustrations of Fe$_3$O$_4$/MWCNTs (left) and PANI/Fe$_3$O$_4$/MWCNTs (right)
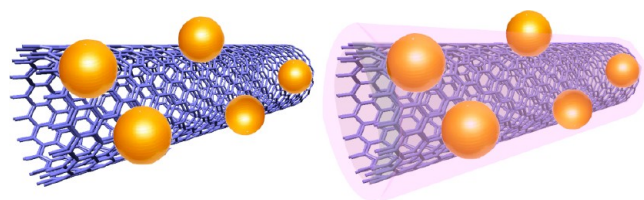
nanotubes (PANI/Fe$_3$O$_4$/MWCNTs, three-phase heterostructures) (Scheme 1) separately to allow a direct comparison of their dielectric properties and microwave absorption. The Fe$_3$O$_4$/MWCNTs were fabricated by the co-precipitation of Fe^{2+} and Fe^{3+}, and an additional process of in situ polymerization of aniline monomer was carried out for obtaining PANI/Fe$_3$O$_4$/MWCNTs. The effects of coated Fe$_3$O$_4$ and PANI on magnetic and dielectric properties were evaluated. The implications of the comparison between two-phase and three-phase heterostructures with respect to their potential applications in electromagnetic shielding and attenuation performance were discussed.

■ RESULTS AND DISCUSSIONS

The Fe$_3$O$_4$/MWCNT heterostructures were achieved via the co-precipitating of Fe^{2+} and Fe^{3+}. For the typical experiment,[25] the as-supplied MWCNTs were processed in concentrated sulfuric acid treatment. The as-treated MWCNTs were dispersed in an aqueous solution, followed by adding NH$_4$Fe(SO$_4$)$_2$·12H$_2$O and (NH$_4$)$_2$FeSO$_4$·6H$_2$O. Upon adding ammonia water, the mixture suspension was applied to vigorous stirring for co-precipitating reaction. The resulting samples (Fe$_3$O$_4$/MWCNTs) were centrifuged, washed with water and ethanol, and dried in an oven. For the fabrication of PANI/Fe$_3$O$_4$/MWCNTs, the as-prepared Fe$_3$O$_4$/MWCNT samples were redispersed in water, followed by adding phosphoric acid and aniline. Ammonium persulfate (APS) aqueous solution was added into the blend suspension for polymerization process. The as-achieved precipitations (PANI/Fe$_3$O$_4$/MWCNTs) were washed with water and ethanol and dried in an oven. The as-prepared samples were carried out on scanning electron microscopy (SEM) and other techniques. Shown in Figure 1 are the typical morphology of the as-received MWCNTs (Figure 1a), as-prepared Fe$_3$O$_4$/MWCNTs (Figure 1b), and PANI/Fe$_3$O$_4$/MWCNTs (Figure 1c), demonstrating larger average diameter observed in the latter because of the existence
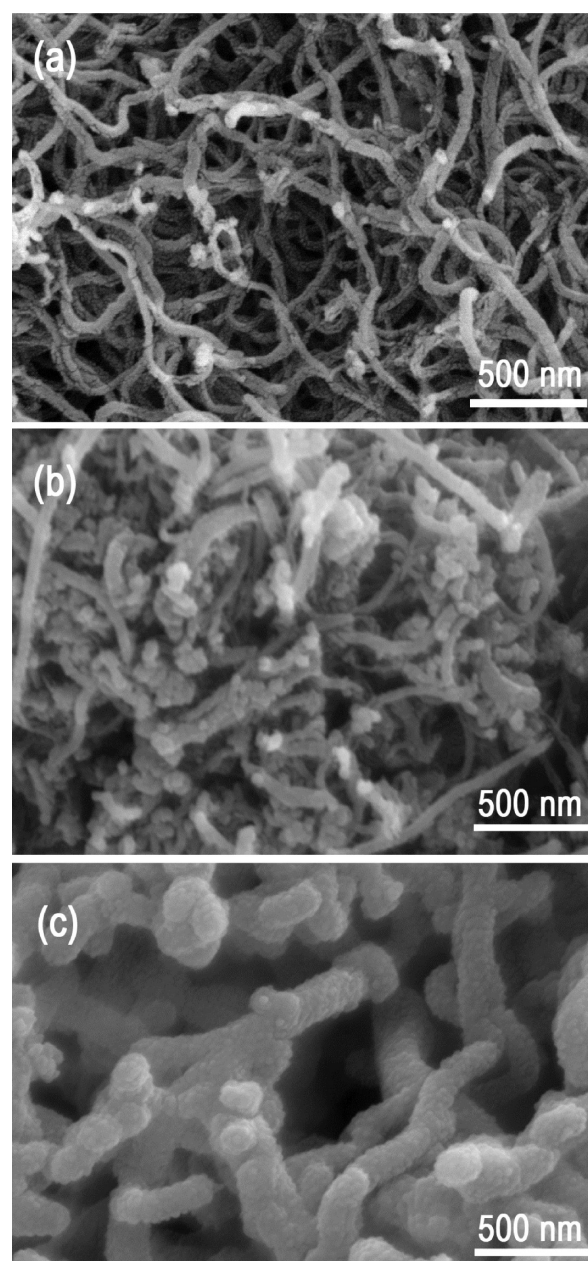
Figure 1. SEM images of (a) the as-received MWCNTs, (b) Fe$_3$O$_4$/MWCNTs, and (c) PANI/Fe$_3$O$_4$/MWCNTs.

of PANI coating. Representative transmission electron microscopy (TEM) images for the Fe$_3$O$_4$/MWCNTs (Figure 2b) and PANI/Fe$_3$O$_4$/MWCNTs (Figure 2c) suggest the Fe$_3$O$_4$ particles are randomly coated on the MWCNT surface as expected. High-resolution TEM images also suggest PANI coating observed in PANI/Fe$_3$O$_4$/MWCNT samples and Fe$_3$O$_4$ particles on the order of 10−20 nm in diameter (Figure 2d), with a lattice spacing of ∼0.3 nm and a corresponding d-spacing of (220) crystal plane (Figure 2e).

The results of X-ray powder diffraction (XRD) for MWCNTs (—), PANI (●●●), Fe$_3$O$_4$/MWCNTs (-●-●), and PANI/Fe$_3$O$_4$/MWCNTs (---) are shown in Figure 3. The characteristic graphitic peak centered at ∼2θ=26.5° indicates that the MWCNTs were well preserved during the synthesis of the heterostructures. According to Fe$_3$O$_4$ in the MDI Jade database (JCPDS No. 89-0691), the characteristic diffraction
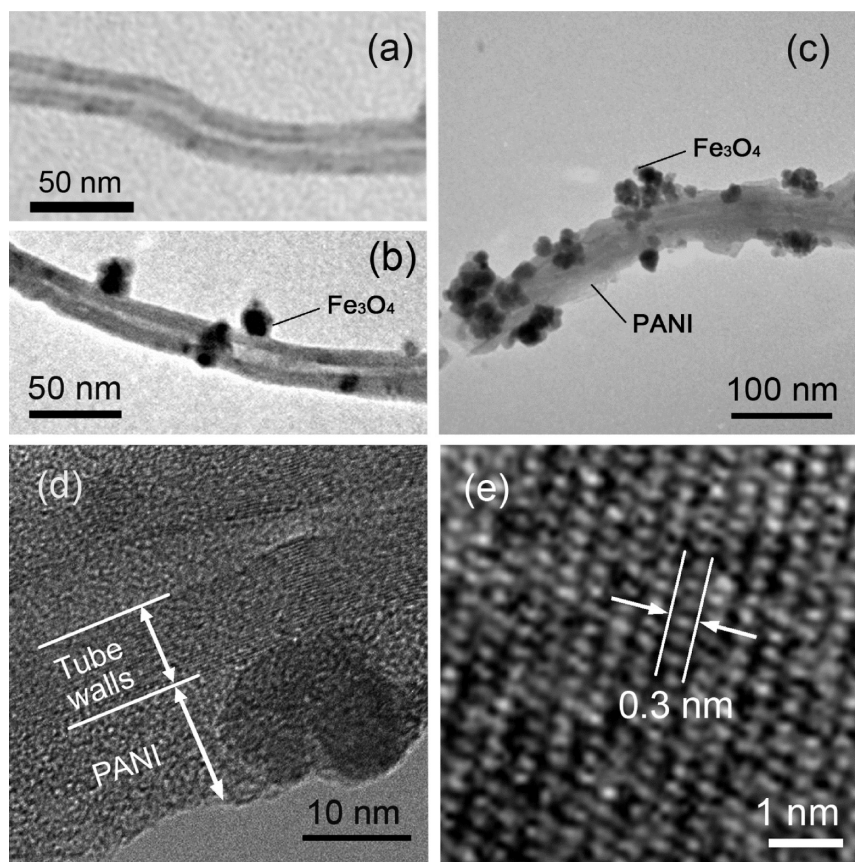
Figure 2. (a) TEM image of the as-received MWCNTs; (b) TEM image of Fe_3O_4/MWCNTs; (c) TEM image of PANI/Fe_3O_4/MWCNTs; (d, e) high-resolution TEM images of PANI/Fe_3O_4/MWCNTs.
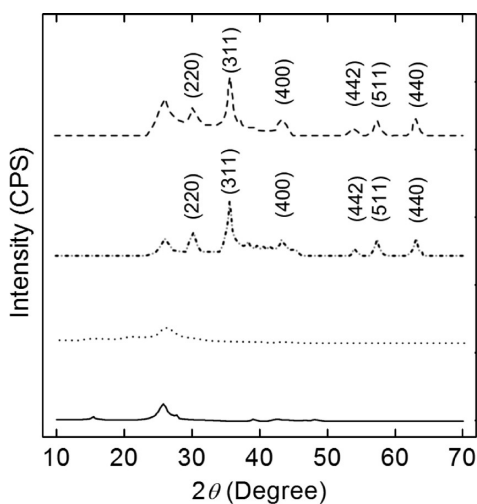
Figure 3. XRD spectra of MWCNTs (—), PANI (•••), Fe_3O_4/MWCNTs (-•-•), and PANI/Fe_3O_4/MWCNTs (---).

Figure 4. Hysteresis loops of Fe_3O_4/MWCNTs (○) and PANI/Fe_3O_4/MWCNTs (△).

peaks centered at 2θ = 30.2, 35.7, 43.3, 53.8, 57.3, and 62.9° are associated with (220), (311), (400), (422), (511), and (440) planes, respectively, no meaningful change before and after the PANI polymerization (Figure 3). Figure 4 exhibits the hysteresis loops of Fe_3O_4/MWCNTs (○) and PANI/Fe_3O_4/MWCNTs (△), suggesting saturation magnetizations of 31.4 and 9.4 emu/g, respectively. The addition coating of PANI reduces the effective mass/volume percentage of Fe_3O_4 in the nanocomposites with the same filler loading, thus relatively less hysteresis observed. The saturation magnetization produced by
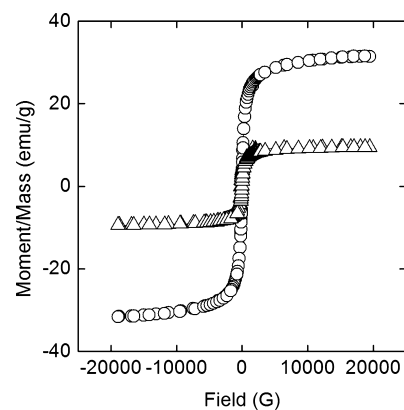
Fe_3O_4 sufficiently improves the low-frequency complex permeability of the heterostructures. However, improved magnetic properties is favorable for natural resonance loss and eddy current loss, leading to enhanced magnetic loss.

The neat PANI and PANI/Fe_3O_4/MWCNTs were applied to Fourier transform infrared spectroscopy (FT-IR). According the results of PANI (•••) and PANI/Fe_3O_4/MWCNTs (—) in Figure 5, the peaks at 1600 and 1430 cm^{-1} are assigned to the stretching vibration of C=N in quinoid ring and C=C in benzenoid ring, respectively, in PANI.[26] The peak at 3237 cm^{-1} is attributed to the N–H stretching vibration in PANI.[26] The peaks observed around 3400 and 1700 cm^{-1} in PANI/Fe_3O_4/MWCNTs are associated with O–H and C=O bands in
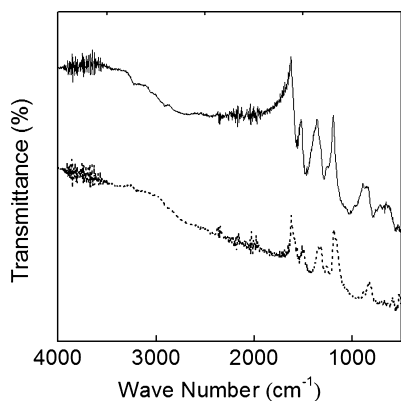
Figure 5. FT-IR spectra of the PANI (•••) and PANI/Fe$_3$O$_4$/MWCNTs (—).

MWCNTs produced during the sulfuric acid treatment.[27] The enhanced peak at 1290 cm^{-1} for the heterostructures is due to the C–N stretching vibration in PANI.[26] The peak around 790 cm^{-1} is assigned to the C–H bending absorption for benzenoid unit of PANI.[26] The Raman spectra of the as-treated MWCNTs (—), Fe$_3$O$_4$/MWCNTs (---), and PANI/Fe$_3$O$_4$/MWCNTs (-•-•) were shown in Figure 6. No meaningful changes of D
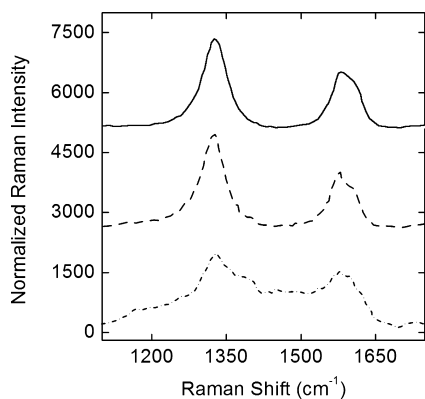

Figure 6. Raman spectra of as-treated MWCNTs (—), Fe$_3$O$_4$/MWCNTs (---), and PANI/Fe$_3$O$_4$/MWCNTs (-•-•).

band (~1320 cm^{-1}) and G band (~1590 cm^{-1}) were observed in the Fe$_3$O$_4$/MWCNTs, compared to the as-treated

MWCNTs. However, the coating of PANI exhibited great influence in the as-achieved PANI/Fe$_3$O$_4$/MWCNTs. After PANI coated, disorder-induced D band was slightly shifted to higher wavenumbers ~1330 cm^{-1}, and peaks at 1168, 1252, 1380, and 1450 cm^{-1}, attributed to PANI, were observed.[28,29]

The wax-based composites were fabricated via compressing at room temperature. The as-prepared Fe$_3$O$_4$/MWCNT powders (20 wt %) were dispersed with paraffin wax (80 wt %) in an ether solution, followed by evaporating the solvent. The dried samples were collected and compressed into a toroidal shape. The relative complex permittivity and permeability of the wax-based composites was confirmed on an Anritsu 37269D vector network analyzer by the coaxial method. As shown in Figure 7a–c, the complex permittivity ($\varepsilon = \varepsilon' - j\varepsilon''$), complex permeability ($\mu = \mu' - j\mu''$) and tangent loss (tan $\delta_e = \varepsilon''/\varepsilon'$, tan $\delta_m = \mu''/\mu'$) of Fe$_3$O$_4$/MWCNT wax composites was observed in 2–18 GHz. Besides a slight peak found at ~7.2 GHz, both real (ε') and imaginary (ε'') permittivity was found to decrease with increasing frequency in the investigated region (Figure 7a). As discussed above, the complex permeability was dominated by the coated Fe$_3$O$_4$ nanoparticles, and a resonance peak mainly associated with the interface between Fe$_3$O$_4$ nanoparticles and MWCNTs (Scheme 2a) was observed at ~8.5 GHz (Figure 7b). The observed dielectric tangent loss (tan δ_e) reaches up to 0.55 at 2 GHz and stays higher than 0.4 over the whole region (Figure 7c), much higher than the magnetic loss, which indicates that dielectric loss makes major contribution to the electromagnetic loss.

Similarly, the wax-based composites filled with PANI/Fe$_3$O$_4$/MWCNTs (20 wt %) were achieved via the combination of mixing and compressing method aforementioned. The same measurement on the complex permittivity and permeability was made on the as-fabricated PANI/Fe$_3$O$_4$/MWCNT wax composites. As shown in Figure 7d, two peaks were observed in the complex permittivity of PANI/Fe$_3$O$_4$/MWCNT composites, which show resonant characteristics.[30] Besides the peak also found in Fe$_3$O$_4$/MWCNT composites (at ~7.2 GHz), the interface between MWCNTs and PANI (Scheme 2c) would generate a heterojunction capacitor, which is possibly responsible to the resonance peak at ~14.1 GHz.[30] On the other hand, decrease values were observed in both real and imaginary permittivity of PANI/Fe$_3$O$_4$/MWCNT composites, compared to Fe$_3$O$_4$/MWCNT ones. On the basis of
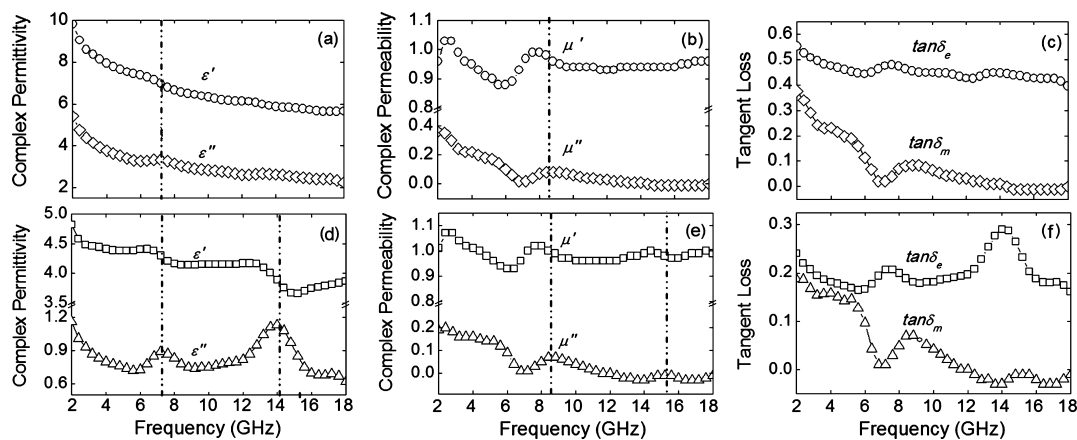

Figure 7. (a) Complex permittivity, (b) complex permeability, and (c) tangent loss of Fe$_3$O$_4$/MWCNT wax composites; (d) complex permittivity, (e) complex permeability, and (f) tangent loss of PANI/Fe$_3$O$_4$/MWCNT wax composites.

6952

dx.doi.org/10.1021/am3021069 | ACS Appl. Mater. Interfaces 2012, 4, 6949–6956

Scheme 2. Illustrations of Interface Effects for (a) Fe$_3$O$_4$/MWCNTs and (c) PANI/Fe$_3$O$_4$/MWCNTs; Contact Resistance for (b) Fe$_3$O$_4$/MWCNTs ($R_{cont} = R_{MWCNT}$ or $= R_{MWCNT} + R_{Fe3O4}$); and (d) PANI/Fe$_3$O$_4$/MWCNTs ($R_{cont} = R_{MWCNT} + R_{PANI}$ or $= R_{MWCNT} + R_{PANI} + R_{Fe3O4}$)
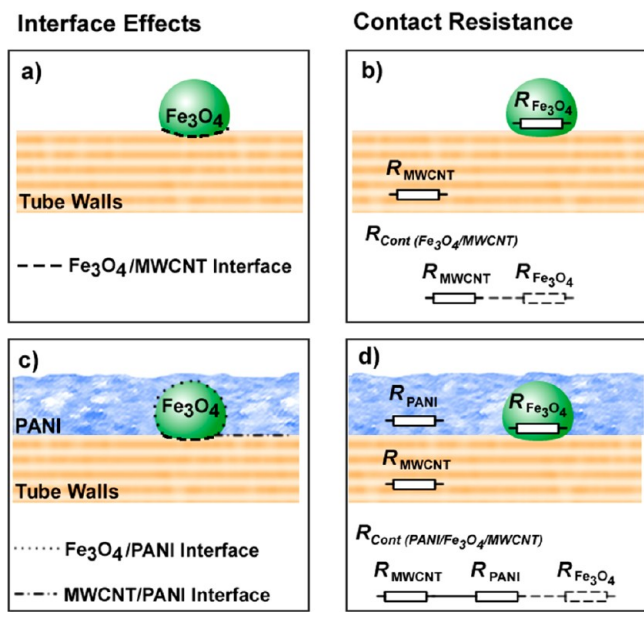
Debye theory on dielectric, imaginary permittivity ε'' is generally known as

$$\varepsilon'' = \frac{\varepsilon_s - \varepsilon_\infty}{1 + \omega^2 \tau^2} \omega\tau + \frac{\sigma}{\omega\varepsilon_0} \qquad (1)$$

where ε_s is the static permittivity, ε_∞ the relative dielectric permittivity at the high-frequency limit, ω the angular frequency, τ the polarization relaxation time, and σ the electrical conductivity. Electrical conductivity is thus considered as a significant factor in the imaginary permittivity. In the CNT-based composites, it's already well-documented that electrical conductivity of the composites is mainly attributed to the electrically conductive network established by CNT aggregations.[31,32] In the PANI/Fe$_3$O$_4$/MWCNT composites here, the PANI layer coated on the MWCNT surface would increase the contact electrical resistance of the CNT network (Scheme 2d), because the fact that PANI possesses lower electrical conductivity than MWCNTs.[24] Therefore, it's reasonable to observe decreased imaginary permittivity in the heterostructures coated by PANI. As shown in Figure 7e, a similar peak at ~8.5 GHz was also observed in the complex permeability of PANI/Fe$_3$O$_4$/MWCNT composites, and an additional peak was found at 15.2 GHz, suggesting the main contribution of the interface between Fe$_3$O$_4$ and PANI (Scheme 2c). These kinds of resonance peaks observed in complex permeability are considered to be associated with local confinement, natural resonance and exchange resonance loss.[18,19] Besides the additional peak, there is only slight change between the complex permeability of PANI/Fe$_3$O$_4$/MWCNT and Fe$_3$O$_4$/MWCNT composites at 2-3 GHz (Figures 7b, e). Although they are different in saturation magnetizations as discussed above, the role of magnetic properties has great influence on the complex permeability in the MHz range rather than GHz range.[33] The tangent loss (tan δ_e) of PANI/Fe$_3$O$_4$/MWCNT composites in Figure 7f shows lower dielectric loss than that of

Fe$_3$O$_4$/MWCNTs, due to the decrease in the electrical conductivity of the PANI-coated CNT network. However, both PANI/Fe$_3$O$_4$/MWCNT and Fe$_3$O$_4$/MWCNT composites exhibit higher dielectric loss than magnetic loss, suggesting major contribution of dielectric loss, different from some of the Fe/CNTs hybrid systems dominated by magnetic loss.[18,19]

Calculation for the microwave absorption of the composites was carried out based on the experimentally determined complex permittivity and permeability. The reflection loss (R_L) can be calculated as[34]

$$R_L = 20\log\frac{|Z_{in} - 1|}{|Z_{in} + 1|} \qquad (2)$$

Here the normalized input impedance Z_{in} of microwave absorption layer is as follow

$$Z_{in} = \sqrt{\frac{\mu_r}{\varepsilon_r}} \tanh\left[j\frac{2\pi}{c} \sqrt{\mu_r \varepsilon_r} f d \right] \qquad (3)$$

where c is the light velocity, f the microwave frequency, d the thickness of the absorber, ε_r and μ_r the complex permittivity and permeability of the composite medium, respectively. In our calculation, d was considered to be 2, 3, 4, and 5 mm, respectively. The evaluated reflection loss of Fe$_3$O$_4$/MWCNT composites coupled with different thicknesses is shown in Figure 8a. It's obviously exhibited that the reflection loss peaks
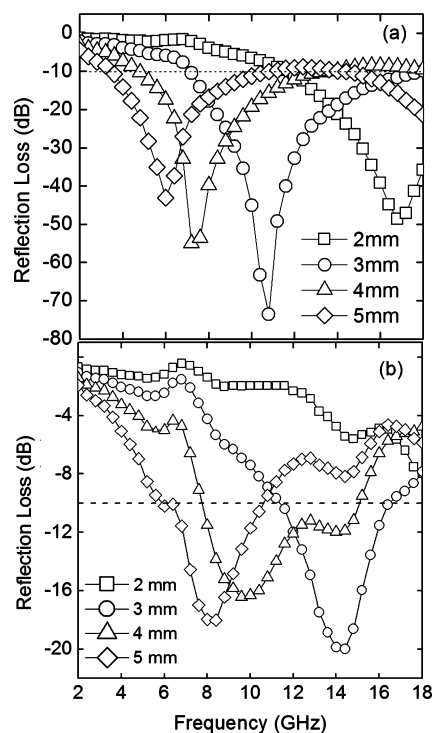
Figure 8. Reflection loss plots of (a) Fe$_3$O$_4$/MWCNT and (b) PANI/Fe$_3$O$_4$/MWCNT wax composites.

shift from higher to lower frequency while the thickness increases, associated with quarter-wavelength attenuation.[35] The Fe$_3$O$_4$/MWCNT composites demonstrate excellent microwave absorption performance with wide absorption bandwidth due to the combined contribution of dielectric and magnetic loss. In the investigated region, the reflection loss peak easily achieves up to 40 dB and the maximum one reaches ~75 dB (3 mm in thickness), much more effective than that of naked CNT

Table 1. Microwave Absorption Performance of Representative CNT-Based Composites

samples in matrices	wt %	max RL value (dB)	d (mm) (RL > 10 dB)	frequency range (GHz) (RL > 10 dB)	effective bandwidth (RL > 10 dB)	frequency range (GHz) (RL > 20 dB)	effective bandwidth (RL > 20 dB)	refs
SWNTs in polyurethane	5	22	2	7.6−9.3	1.7	8.3−9.2	0.9	ref 37
MWNTs in varnish	8	24.27	1	13.2−18	4.8	15−16	1	ref 36
MWCNTs/Fe in epoxy resin	60	39	3.36−5.57			2.04−3.47	1.43	ref 19
MWCNTs/Co in epoxy resin	60	37	4.18−6.82			2.35−3.51	1.16	ref 19
MWCNTs/Ni in epoxy resin	60	37	3.77−6.56			1.83−3.07	1.24	ref 19
MWCNT with Ni in wax	15.6	24.8	1.5	10.5−14.5	4	11.6−12.4	0.8	ref 40
α-Fe@CNT in epoxy resin	20	25	1.2	2−18	16	4.5−5.5; 8.5−11.8	4.3	ref 18
CNTs/CoFe$_2$O$_4$ in epoxy resin	8	18	1.4	6.5−-13.5	7			ref 39
carbon-coated Ni in wax	50	32	2	11.2−15.5	4.3	12.5−13.7	1.2	ref 41
Fe@CNT in epoxy resin	10	31.71	1	11.8−14.7	2.9	12.5−13.5	1	ref 20
MWCNT-La(NO$_3$)$_3$ in PVC	6	28	2	7−17.8	10.8	12.3−14.3	2	ref 42
Fe$_3$O$_4$/MWCNT in wax	20	75	3	7−18	11	8.3−13.6	5.3	this work
PANI/Fe$_3$O$_4$/MWCNT in wax	20	16	4	8−15	7			this work

composites dominated by dielectric loss.[36−38] On the other hand, broadband microwave absorption based on CNT-filled composites is highly pursued for widening effective attenuation. For example, in the work by Chen and coworkers,[37] polymeric composites filled with neat CNT (5 wt %) exhibited an absorption bandwidth ∼1.7 GHz (R_L > 10 dB). Wen et al.[19] reported epoxy composites filled with Fe, Co and Ni coated MWCNTs separately (60 wt %) with an absorption bandwidth ∼1.1−1.5 GHz (R_L > 20 dB). A much broadened absorption bandwidth was achieved in the epoxy composites embedded with Fe-filled CNTs (20 wt %),[18] showing absorption bandwidth of 16 GHz for R_L > 10 dB and 4.3 GHz for R_L > 20 dB, respectively. In this work, wide bandwidth with effective absorption (R_L > 10 dB) from 7 GHz to 18 GHz (11 GHz in width) and highly effective absorption (R_L > 10 dB) from 8.3 GHz to 13.6 GHz (5.3 GHz in width), respectively, was observed in the Fe$_3$O$_4$/MWCNT composites, competitive to, or even much wider than, the results from the CNT-based composites in the literature (Table 1).

The same calculated process was also applied to PANI/Fe$_3$O$_4$/MWCNT composites. The results suggest PANI/Fe$_3$O$_4$/MWCNT composites less effective in microwave absorption by comparing to Fe$_3$O$_4$/MWCNT ones (Figure 8b), mainly associated with the decreased dielectric loss due to the PANI layer. Generally, microwave absorption depends on the impedance match conditions of the interfaces between the fillers and air.[4] Thus, the existence of PANI coatings with a different electrical conductivity and dielectric properties could change the impedance between MWCNTs and air, leading to different microwave absorption performance between PANI/Fe$_3$O$_4$/MWCNT and Fe$_3$O$_4$/MWCNT heterostructures. However, the best microwave absorption width of the PANI/Fe$_3$O$_4$/MWCNT composites is still larger than 7 GHz, also wider than some results from the CNT-based composites (Table 1).

The comparison here suggests that the microwave absorption with respect to both dielectric and magnetic loss exhibits much

more effective performance. In this regard, the combination of magnetic materials with dielectric materials has been proved to provide a promising arena for achieving high performance microwave-absorption materials. Typically, two-phase heterostructures, such as Fe$_3$O$_4$/MWCNTs and Fe@CNTs, by introducing magnetic materials onto/into carbon nanotubes exhibit enhanced resonance at the introduced interfaces, and thus improve microwave absorption efficiency and related effective bandwidth. On the other hand, electrical properties based on electrical conductivity could be a significant role in both dielectric properties and microwave absorption. In the multi-phase heterostructures, such as PANI/Fe$_3$O$_4$/MWCNTs, the polymer coating with lower electrical conductance probably limits the performance of dielectric loss. Also, the materials with good electrical conductivity may produce skin effect and additional reflection at the surface between materials and air,[43] which offers effective electromagnetic attenuation. Thus, the PANI/Fe$_3$O$_4$/MWCNTs based on the PANI coating may result in decreased microwave absorption efficiency. Although the microwave absorption was observed to be influenced by PANI coating, PANI is an effective coating preventing Fe$_3$O$_4$ from further oxidation,[25] thus enhancing the stability of Fe$_3$O$_4$ in the heterostructures. Moreover, introduction of light-weight PANI may improve the interface between carbon nanotubes and matrices, which may result in the light-weight composites of better matrix−filler compatibility.[44] As already suggested by the results here, Fe$_3$O$_4$/MWCNTs, superior to PANI/Fe$_3$O$_4$/MWCNTs, are excellent fillers for enhanced microwave absorption based on both improved dielectric and magnetic properties. The introduction of a second or multiple phases in/onto carbon materials with a specific approach is a significant role in design and fabrication of high-performance microwave absorption composites.

CONCLUSIONS

Fe$_3$O$_4$/MWCNT and PANI/Fe$_3$O$_4$/MWCNT heterostructures were fabricated for direct comparison in dielectric properties and microwave absorption performance, and both their wax composites exhibited highly efficient microwave attenuation. The interface introduced by Fe$_3$O$_4$ generated resonance in complex permittivity and permeability as well as sufficiently enhanced magnetic loss, resulting in enhancing microwave absorption performance and widening effective absorption bandwidth. The introduced PANI coating was found to decrease dielectric loss due to the reduction of electrical conductivity for CNT conductive network. Implication of the comparison results suggests Fe$_3$O$_4$/MWCNTs are greatly effective fillers in highly effective electromagnetic shielding and attenuation.

EXPERIMENTAL SECTION

Materials. MWCNT fabricated by the catalytic decomposition of CH$_4$ was purchased from Shenzhen Nanotech Port Co. Ltd. (China). The as-supplied MWCNTs (~1 g) were dispersed in concentrated sulfuric acid with vigorous stirring for 2 h at 100 °C, followed by filtration and washing with deionized water until neutral pH value in the washing solution. Sulfuric acid was obtained from Beijing Chemical factory. Ferrous ammonium sulfate ((NH$_4$)$_2$FeSO$_4$·6H$_2$O) was provided by Dongli District of Tianjin Tianda Chemical Reagent. Ferric ammonium sulfate (NH$_4$Fe(SO$_4$)$_2$·12H$_2$O) was supplied by Bazhou Chemical factory of Tianjin quartz factory. Ethanol was obtained from Tianjin Fu Yu Fine Chemical Co. Ltd. Ammonia water was supplied by Qiqihaer Tianyuan Water Company. Aniline provided by Tianli Tianjin Chemical Reagent Co. Ltd was distilled in vacuum before use.

Measurement. Fourier transform infrared spectroscopy (FT-IR) was carried out on a Nicolet 8700 FT-IR system. X-ray powder diffraction (XRD) measurements were performed on an XPert PRO system (Cu−Kα). Magnetic properties were measured by a Lakeshore 7407 vibrating sample magnetometer (VSM). Scanning electron microscopy (SEM) images were performed on a Hitachi S-4300 field-emission SEM system. Transmission electron microscopy (TEM) images on a JEM-2100 TEM system, coupled with the use of carbon- or holey carbon-coated copper grids. The lattice measurement was obtained by the division of the width for 20 stripes. The relative permittivity and permeability were measured on an Anritsu 37269D vector network analyzer by the coaxial method. Raman spectra were obtained on a HORIBA Jobin Yvon HR800 Raman spectromater equipped with a Spectra-Physics Ar−Kr laser source for 647 nm excitation and on Olympus BX-41 microscope.

Fe$_3$O$_4$/MWCNT heterostructures. In a typical fabrication experiment,[25] the as-treated MWCNTs (100 mg) were dispersed in aqueous solution, followed by adding NH$_4$Fe(SO$_4$)$_2$·12H$_2$O (0.793 g) and (NH$_4$)$_2$FeSO$_4$·6H$_2$O (0.322 g). The mixture suspension was sonicated for 10 min, whereas NH$_3$·H$_2$O (5 ml, 25 wt %) was dropwise added into the suspension. After sonication, vigorous stirring was applied to the mixture suspension for co-precipitating reaction at 50 °C for 30 min. The resulting suspension was centrifuged and the precipitations were collected, followed by washing with deionized water and ethanol and drying in an oven (80−100 °C).

PANI/Fe$_3$O$_4$/MWCNT Heterostructures. For fabrication of PANI/Fe$_3$O$_4$/MWCNT multiphase heterostructure,[25] a portion of the as-prepared Fe$_3$O$_4$/MWCNT heterostructure (106 mg) was dispersed in 30 ml deionized water. Phosphoric acid (0.1 ml, 85 wt %) and aniline (0.2 ml) were subsequently added under stirring condition. Until homogenous suspension was achieved, ammonium persulfate (APS) aqueous solution (0.466 g of APS in 20 mL of deionized water) was dropwise added to the suspension. The polymerization process was applied in an ice bath for 6 h under vigorous stirring. The resulting precipitations were washed with deionized water and ethanol, followed by drying in an oven (60−70 °C).

Wax Composites. In a typical experiment, Fe$_3$O$_4$/MWCNTs (20 wt %) and paraffin wax (80 wt %) were added into pre-heated ether solution at 70 °C under vigorous stirring. After the ether was completely evaporated, the mixture was cooled to room temperature. A portion of the resulting mixture was pressed into toroidal shape (Φ_{out}, 7.03 mm; Φ_{in}, 3.00 mm).[35] Similarly, PANI/Fe$_3$O$_4$/MWCNT wax composites with the same weight ratio (20 wt %) were fabricated via the process as described above.

AUTHOR INFORMATION

Corresponding Author

*E-mail: caomaosheng@bit.edu.cn (M.-S.C.); dexterquest@gmail.com (W.-L.S.); yuanjie4000@163.com (J.Y.).

Notes

The authors declare no competing financial interest.

REFERENCES

(1) Yang, Y. L.; Gupta, M. C. *Nano Lett.* **2005**, *5*, 2131−2134.
(2) Li, N.; Huang, Y.; Du, F.; He, X. B.; Lin, X.; Gao, H. J.; Ma, Y. F.; Li, F. F.; Chen, Y. S.; Eklund, P. C. *Nano Lett.* **2006**, *6*, 1141−1145.
(3) Mahmoodi, M.; Arjmand, M.; Sundararaj, U.; Park, S. *Carbon* **2012**, *50*, 1455−1464.
(4) Cao, M. S.; Song, W. L.; Hou, Z. L.; Wen, B.; Yuan, J. *Carbon* **2010**, *48*, 788−796.
(5) Watts, P. C. P.; Hsu, W. K.; Barnes, A.; Chambers, B. *Adv. Mater.* **2003**, *15*, 700−703.
(6) Thomassin, J. M.; Vuluga, D.; Alexandre, M.; Jerome, C.; Molenberg, I.; Huynen, I.; Detrembleur, C. *Polymer* **2012**, *53*, 169−174.
(7) Thomassin, J. M.; Huynen, I.; Jerome, R.; Detrembleur, C. *Polymer* **2010**, *51*, 115−121.
(8) Dang, Z. M.; Yao, S. H.; Yuan, J. K.; Bai, J. B. *J. Phys. Chem. C* **2010**, *114*, 13204−13209.
(9) Arjmand, M.; Mahmoodi, M.; Gelves, G. A.; Park, S.; Sundararaj, U. *Carbon* **2011**, *49*, 3430−3440.
(10) Logakis, E.; Pandis, C.; Peoglos, V.; Pissis, P.; Pionteck, J.; Potschke, P.; Micusik, M.; Omastova, M. *Polymer* **2009**, *5*, 5103−5111.
(11) Liu, Z. F.; Bai, G.; Huang, Y.; Ma, Y. F.; Du, F.; Li, F. F.; Guo, T. Y.; Chen, Y. S. *Carbon* **2007**, *45*, 821−827.
(12) Saini, P.; Choudhary, V.; Singh, B. P.; Mathur, R. B.; Dhawan, S. K. *Mater. Chem. Phys.* **2009**, *113*, 919−926.
(13) Peng, Z. H.; Peng, J. C.; Peng, Y. F.; Ou, Y. Y.; Ning, Y. T. *Phys. Lett. A* **2008**, *372*, 3714−3718.
(14) Yuan, B. Q.; Yu, L. M.; Sheng, L. M.; An, K.; Zhao, X. L. *J. Phys. D: Appl. Phys.* **2012**, *45*, 235108.
(15) Su, Q. M.; Li, J.; Zhong, G.; Du, G. H.; Xu, B. S. *J. Phys. Chem. C* **2011**, *115*, 1838−1842.
(16) Zhao, D. L.; Zhang, J. M.; Li, X.; Shen, Z. M. *J. Alloys Compd.* **2010**, *505*, 712−716.
(17) Lin, H. Y.; Zhu, H.; Guo, H. F.; Yu, L. F. *Mater. Res. Bull.* **2008**, *43*, 2697−2702.
(18) Che, R. C.; Peng, L. M.; Duan, X. F.; Chen, Q.; Liang, X. L. *Adv. Mater.* **2004**, *16*, 401−405.
(19) Wen, F. S.; Zhang, F.; Liu, Z. Y. *J. Phys. Chem. C* **2011**, *115*, 14025−14030.
(20) Zhao, D. L.; Li, X.; Shen, Z. M. *J. Alloys Compd.* **2009**, *471*, 457−460.
(21) Kim, H. M.; Kim, K.; Lee, C. Y.; Joo, J.; Cho, S. J.; Yoon, H. S.; Pejakovic, D. A.; Yoo, J. W.; Epstein, A. J. *Appl. Phys. Lett.* **2004**, *84*, 589−591.

(22) Che, R. C.; Liang, C. Y.; Shi, H. L.; Zhou, X. G.; Yang, X. N. *Nanotechnology* **2007**, *18*, 300755.

(23) Zhao, C. Y.; Zhang, A. B.; Zheng, Y. P.; Luan, J. F. *Mater. Res. Bull.* **2012**, *47*, 217−221.

(24) Yun, J.; Kim, H. *Polym. Bull.* **2012**, *68*, 561−573.

(25) Liu, Z.; Wang, J.; Xie, D. H.; Chen, G. *Small* **2008**, *4*, 462−466.

(26) Amrithesh, M.; Aravind, S.; Jayalekshmi, S.; Jayasree, R. S. *J. Alloys Compd.* **2008**, *449*, 176−179.

(27) Kastner, J.; Pichler, T.; Kuzmany, H.; Curran, S.; Blau, W.; Weldon, D. N.; Delamesiere, M.; Draper, S.; Zandbergen, H. *Chem. Phys. Lett.* **1994**, *221*, 53−58.

(28) Salvatierra, R. V.; Oliveira, M. M.; Zarbin, A. J. G. *Chem. Mater.* **2010**, *22*, 5222−5234.

(29) Huang, F.; Vanhaecke, E.; Chen, D. *Catal. Today* **2010**, *150*, 71−76.

(30) Shi, X. L.; Cao, M. S.; Yuan, J.; Zhao, Q. L.; Kang, Y. Q.; Fang, X. Y.; Chen, Y. J. *Appl. Phys. Lett.* **2008**, *93*, 183118.

(31) Dang, Z. M.; Wang, L.; Yin, Y.; Zhang, Q.; Lei, Q. Q. *Adv. Mater.* **2007**, *19*, 852−857.

(32) Kaiser, A. B.; Skalova, V. *Chem. Soc. Rev.* **2011**, *40*, 3786−3801.

(33) Liu, S. H.; Liu, J. M.; Dong, X. L. *Electromagnetic Interference Shielding and Microwave Absorption Materials*; Chemical Industrial Press: Beijing, 2007.

(34) Singh, P.; Babbar, V. K.; Razdan, A.; Puri, R. K.; Goel, T. C. *J. Appl. Phys.* **2000**, *87*, 4362−4368.

(35) Song, W. L.; Cao, M. S.; Wen, B.; Hou, Z. L.; Cheng, J.; Yuan, J. *Mater. Res. Bull.* **2012**, *47*, 1747−1754.

(36) Fan, Z. J.; Luo, G. H.; Zhang, Z. F.; Zhou, L.; Wei, F. *Mater. Sci. Eng., B* **2006**, *132*, 85−89.

(37) Liu, Z. F.; Bai, G.; Huang, Y.; Li, F. F.; Ma, Y. F.; Guo, T. Y.; He, X. B.; Lin, X.; Gao, H. J.; Chen, Y. S. *J. Phys. Chem. C* **2007**, *111*, 13696−13700.

(38) Song, W. L.; Cao, M. S.; Hou, Z. L.; Yuan, J.; Fang, X. Y. *Scripa Mater.* **2009**, *61*, 201−204.

(39) Che, R. C.; Zhi, C. Y.; Liang, C. Y.; Zhou, X. G. *Appl. Phys. Lett.* **2006**, *88*, 033105.

(40) Deng, L. J.; Han, M. G. *Appl. Phys. Lett.* **2007**, *91*, 023119.

(41) Zhang, X. F.; Dong, X. L.; Huang, H.; Liu, Y. Y.; Wang, W. N.; Zhu, X. G.; Lv, B.; Lei, J. P.; Lee, C. G. *Appl. Phys. Lett.* **2006**, *89*, 053115.

(42) Hou, C. L.; Li, T. H.; Zhao, T. K.; Cheng, T.; Zhang, W. J.; Li, G. G. *Mater. Lett.* **2012**, *67*, 84−87.

(43) Chung, D. D. L. *Carbon* **2012**, *50*, 3342−3353.

(44) Jin, R. G.; Hua, Y. Q. *Polymer Physics*; Chemical Industrial Press: Beijing, 2008.